Catalysis Today 179 (2012) 140–148

Contents lists available at ScienceDirect

Catalysis Today

journal homepage: www.elsevier.com/locate/cattod

Effect of vanadium dispersion and of support properties on the catalytic activity of V-containing silicas

Marco Piumetti[a], Barbara Bonelli[a,*], Pascale Massiani[b], Stanislaw Dzwigaj[b], Ilenia Rossetti[c], Sandra Casale[b], Marco Armandi[a], Cyril Thomas[b], Edoardo Garrone[a]

[a] Department of Materials Science and Chemical Engineering and INSTM Unit – Torino Politecnico, Politecnico di Torino, Corso Duca degli Abruzzi 24, I-10129 Turin, Italy
[b] UPMC, Université Pierre et Marie Curie (Paris VI), CNRS-UMR 7197, Laboratoire de Réactivité de Surface, 4 Place Jussieu, F-75005 Paris, France
[c] Dipartimento CFE, Università di Milano, ISTM-CNR and INSTM Unit, via C. Golgi 19, I-20133 Milano, Italy

ARTICLE INFO

Article history:
Received 15 April 2011
Received in revised form 16 June 2011
Accepted 17 June 2011
Available online 31 July 2011

Keywords:
Vanadium-containing mesoporous catalysts
V-SBA-15
V-MCF
Direct synthesis
Dichloromethane decomposition
Propane ODH

ABSTRACT

Two V-SBA-15 and V-MCF materials (containing about 2.5 wt.% vanadium) were prepared by direct synthesis and tested as catalysts in the decomposition of the most stable chlorinated-alkane, dichloromethane (a total oxidation reaction) and in the oxidative dehydrogenation (ODH) of propane (a partial oxidation reaction). Comparison was made with: (i) two V-SBA-15 and V-MCF materials prepared by "traditional" impregnation method and (ii) a non-porous V-SiO_2 catalyst prepared by flame pyrolysis. All catalysts tested had a vanadium content of about 2.5 wt.%. Samples properties were investigated by means of complementary techniques (TEM, IR and DR UV–vis spectroscopies, N_2 sorption at −196 °C) in order to find possible correlations between catalytic properties of the studied materials and their different physico-chemical features. It is shown that direct synthesis allows a better vanadium dispersion to be achieved, a feature that positively affects catalytic performances in both total and partial oxidations. The different porous networks of the SBA-15 and MCF supports also play an important role on catalytic activity: both V-SBA-15 samples gave better results in dichloromethane decomposition, whereas both V-MCF samples were more selective in propane ODH. The latter findings are ascribed to different molecules diffusion and residence time inside the channels of either SBA-15 or MCF networks.

1. Introduction

Vanadium-based catalysts are an important class of materials effective in many oxidation reactions, which can be kinetically modelled according to a Mars–van Krevelen (MvK) mechanism based on reduction and subsequent re-oxidation of vanadium [1–3]. Vanadium oxides (VO_x) are used in several industrial processes, such as sulphuric acid production, oxidation of *o*-xylene to phthalic anhydride, ammoxidation of alkyl aromatics to aromatic nitriles and selective reduction (SCR) of NO_x with ammonia [4]. Many other reactions may also occur over V-based systems, including dichloromethane oxidation (a probe reaction for chlorinated volatile organic compounds decomposition) [5], methanol oxidation, carbon monoxide oxidation and partial oxidation of hydrocarbons [6]. Furthermore, supported VO_x are well known to be both active and selective catalysts in the oxidative dehydrogenation (ODH) of light alkanes, basically ethane and propane [7]. The latter reaction would offer an attractive alternative route to olefins (e.g. propene), because the overall reaction pathway is exothermic and the thermodynamic constraints of non-oxidative routes are overcome [8,9]. On the other hand, the need for olefins is progressively growing, especially as far as propene is concerned, leading to the necessity of alternative production processes [7–9]. V-based catalysts mostly consist of a VO_x phase deposited on oxide supports, like SiO_2, Al_2O_3, TiO_2 and ZrO_2 [4]. The support itself is known to play an important role during catalytic reactions, since it affects not only the dispersion of the active phase, but also the nature of active centres (i.e. reactivity, acidity, accessibility, etc.) as well as mass/heat transfer phenomena [5,6,8–10]. After the discovery of ordered mesoporous materials with large surface area and wide pores in the early 1990s, an important research line has concerned the widening of pores in the mesoporous range, in order to favour both active phase dispersion and molecular diffusion inside the support framework [11]. In this respect, SBA-15 and MCF (Mesocellular Foams) materials, which are characterized by wide and uniform pores size, thick walls and high surface area, allow a large concentration of accessible, isolated and well defined vanadium active sites to be obtained [12,13]. Although V-based catalysts are usually prepared by impregnation, it has been observed that both V-SBA-15 [5,13,14] and V-MCF [12,13] materials prepared by direct synthesis exhibit larger surface

* Corresponding author. Tel.: +39 011 5644719; fax: +39 011 5644699.
E-mail address: barbara.bonelli@polito.it (B. Bonelli).

0920-5861/$ – see front matter © 2011 Elsevier B.V. All rights reserved.
doi:10.1016/j.cattod.2011.06.028

area, better dispersion and reducibility of V species, and so offer superior catalytic performances in oxidation reactions. In the present paper, the effect is studied of both V dispersion (highly dispersed VO_x species *versus* micro-crystalline V_2O_5) and support properties (surface area, structure, etc.) as it concerns both dichloromethane conversion (i.e. total oxidation) and propane ODH (i.e. selective oxidation). Two V-SBA-15 and V-MCF mesoporous catalysts (containing *ca.* 2.5 wt.% V) were prepared by direct synthesis; their catalytic performances and physico-chemical properties where compared with those of other materials with similar V content, but prepared by different ways: (i) two impregnated samples (referred to as V-SBA-15-i and V-MCF-i, respectively) and (ii) a non-porous sample obtained by flame pyrolysis (V-SiO_2), a high temperature synthesis technique allowing superior V dispersion to be achieved [8].

2. Experimental

2.1. Materials preparation

Unless otherwise specified, all ACS grade reagents were from Sigma–Aldrich S.r.l. (Milan, Italy).

V-SBA-15 sample was prepared by adding a proper amount of V-precursor during SBA-15 hydrothermal synthesis [5], in order to favour entrance of vanadium into silica walls. More specifically, 4 g $EO_{20}PO_{70}EO_{20}$ (Pluronic P123) and 0.227 g CTMACl (cetyltrimethylammonium chloride) were dissolved into 150 mL water and hydrochloric acid (2 M) to prepare "solution I"; "solution II" was prepared by mixing 0.14 g V_2O_5, 30% H_2O_2, and H_2O (molar ratios H_2O_2:V:H_2O = 1.7:0.06:106), and stirring at 70 °C until the solution turned orange-brown. Afterwards, "solution II" and 9.1 mL TEOS (tetraethoxysilane) were added to "solution I", then stirred at room temperature for 5 h; the solid was recovered by filtration, washed with distilled water, dried overnight and calcined at 500 °C for 6 h.

V-MCF sample was obtained by a novel direct synthesis method [12] by controlling the pH during the synthesis, otherwise V incorporation inside silica does not occur: 4.0 g Pluronic P123 and 2.0 g TMB (1,3,5-trimethylbenzene) were dissolved in 30 mL water and stirred at room temperature for 5 h. Afterwards, 9.0 g TEOS and 0.18 g NH_4VO_3 (ammonium metavanadate) were added to the solution. A 0.20 M HCl aqueous solution was then added drop-wise to the mixture until pH reached a value close to 3.0. After stirring at 40 °C for 24 h at constant pH, the solution was transferred into a Teflon autoclave and aged at 100 °C for 24 h. The obtained solid was filtered off, washed with bi-distilled water and dried overnight at 100 °C under static conditions. Finally, the occluded organic phase was removed by 5 h calcination at 600 °C in air.

For comparison, two samples with similar V-contents (V-SBA-15-i and V-MCF-i) were synthesized by impregnation with NH_4VO_3 aqueous solution of SBA-15 and MCF supports, respectively, followed by drying and calcination at 600 °C. Impregnation was carried out in water, although better vanadium dispersion may be obtained with alcohols [15], in order to use the same solvent as the direct synthesis procedure.

A non-porous catalyst (V-SiO_2) was prepared by flame pyrolysis method [8]. Further detailed description of the synthesis procedures and of the effect of the main operating parameters on catalysts properties can be found in Refs. [5,8,12].

2.2. Materials characterization

V-content was determined by energy dispersive X-ray spectroscopy (EDS) analysis onto 10–50 nm diameter spots (Oxford 7353 probe on a LEO 1450 VP microscope).

BET (Brunauer–Emmett–Teller) specific surface area (S_{BET}) was measured by N_2 adsorption/desorption isotherms at −196 °C on *ca.* 30 mg sample previously outgassed at 150 °C for 5 h in order to remove molecular water and other atmospheric contaminants (Quantachrome Autosorb 1). Pores size distributions (PSDs) were evaluated by either applying the Barrett–Joyner–Halenda (BJH) algorithm to isotherms desorption branch (SBA-15 materials) or according to the modified Broekhoff de Boer (BdB) method by using the Hill's approximation for the adsorbed layer thickness (MCF materials) [16].

Samples morphology was investigated by Transmission Electron Microscopy (TEM, JEM 2011 operating at 200 kV).

For H_2-TPR (Temperature Programmed Reduction) experiments, *ca.* 100 mg sample was placed inside a quartz micro-reactor, then contacted with the reducing flowing gas (5% molar H_2 in Ar, 40 mL min^{-1}) and heated in the 20–1000 °C temperature range (heating rate: 10 °C min^{-1}), while recording H_2 consumption by using a TCD (Thermal Conductivity Detector); a gas condenser operated at −196 °C and placed prior the TCD was used to remove the water possibly formed during reduction.

For infra-red (IR) measurements in the low wavenumbers range, powder samples were mixed with optical-grade KBr and Fourier Transform IR (FT-IR) spectra were collected at 2 cm^{-1} resolution on a Bruker Equinox 55 FT-IR spectrophotometer, equipped with a MCT detector.

Diffuse reflectance (DR) UV–vis spectra were recorded on *ca.* 200–300 mg powder samples pre-outgassed for 2 h at 300 °C (CARY-500 UV–vis–NIR spectrophotometer equipped with an integrating sphere, Varian Instrument).

2.3. Catalytic activity tests

2.3.1. Dichloromethane decomposition

Catalytic tests were carried out in a continuous quartz tubular reactor (7 mm i.d.) heated by an electric furnace [13]. In a typical experiment, *ca.* 70 mg sample was activated at 500 °C for 1 h in air (41 mL min^{-1}) before each run. The gas flow was then switched from air to the reactive mixture (1000 ppm CH_2Cl_2 in air, VVH = 21,000 h^{-1}) and catalytic activity was measured in the 200–500 °C temperature range. The outlet gas composition was analyzed by an on-line gas chromatograph (PERICHROM, PR 2100) with two detection lines: (i) that for analysis of organic compounds was equipped with a capillary column and a flame ionization detector (FID); (ii) that for CO_x detection was equipped with a succession of a Porapak-Q (for back-flush) and a MS-5A columns, and a thermal conductivity detector (TCD). Dichloromethane conversion (%) was calculated as moles of CH_2Cl_2 converted over moles of CH_2Cl_2 fed. The selectivity to each *i*th product was calculated as the ratio between moles of produced *i*th species and moles of converted CH_2Cl_2, normalized to the respective stoichiometric coefficients.

2.3.2. Oxidative dehydrogenation of propane

ODH catalytic tests were carried out in a continuous U-type quartz reactor (10 mm i.d.). Prior to each run, *ca.* 0.1 g catalyst was activated for 1 h in He (30 mL min^{-1}) at 550 °C (2 °C min^{-1}), afterwards temperature was decreased to 375 °C. The composition of reactants mixture was as follows: 6.6% C_3H_8 and 2.3% O_2 in He; total flow rate 15 mL min^{-1}. After the reaction mixture was contacted to the catalyst at 375 °C, temperature was increased stepwise up to 550° (25 °C per step) and maintained constant for 1 h at each reaction step. The outlet gas composition was analyzed by means of a Varian 4900 μ-GC (Micro Gas-Chromatograph) using three different columns (5A molecular sieve, Poraplot-Q and CPSil-5) for complete detection of the effluent products. Carbon and oxygen balances were found to be 100 ± 2%. The propane conversion levels were estimated on the basis of the disappearance of propane:

Table 1
Catalytic data of dichloromethane decomposition, as measured with V-containing catalysts at 500 °C (time on stream = 10 min).

Sample	CH_2Cl_2 conversion (%)	CO_2 selectivity[a] (%)
V-SBA-15	68	95
V-SBA-15-i	31	48
V-MCF	52	75
V-MCF-i	23	45
V-SiO_2	43	65

[a] CO_2 was the only product measured in aerobic conditions with the adopted experimental set up; the "missing products" could involve coke and/or adsorbed compounds.

X C_3H_8 (%) = $(([C_3H_8]_{inlet} - [C_3H_8]_{outlet})/[C_3H_8]_{inlet}) \times 100$, where X C_3H_8, $[C_3H_8]_{inlet}$ and $[C_3H_8]_{outlet}$ are the conversion of propane and the propane concentrations measured at the inlet and the outlet of the reactor, respectively. The selectivity in propene was calculated as SA_i (%) = $(n_i\,[A_i]/(\Sigma n_i\,[A_i]) \times 100)$, where n_i, $[A_i]$, and SA_i are the number of carbon atoms and the concentration in the A_i product, and the selectivity in the A_i product, respectively.

A blank experiment was run with quartz wool in the reactor, in order to test thermal ODH: propane conversion was 0.4% at 400 °C and increased to 2.6% at 550 °C. In the same temperature interval, the highest selectivity to propene was reached at 550 °C and was, however, limited to 13%, the main products being CO_x. Above 500 °C, traces of methane and ethane were observed, due to propane cracking.

3. Results and discussion

3.1. Catalytic activity towards CH_2Cl_2 oxidative decomposition

Fig. 1a and b reports the catalytic activity for the oxidative decomposition of dichloromethane in the 200–500 °C temperature range and Table 1 summarizes the values of both CH_2Cl_2 conversion and selectivity to CO_2 as obtained at 500 °C. Both SBA-15 and MCF pure silicas tested as blanks did not show any catalytic activity. All V-containing catalysts exhibited stable CH_2Cl_2 conversions in the explored temperatures range (time on stream = 2 h) and almost constant selectivity. After reaction, the samples were reactivated at 500 °C and several reaction-cycles were performed: catalysts gave highly reproducible performances. In fair agreement with literature [17,18], by-products were mainly HCl, the most thermodynamically favoured compound at high temperature and Cl_2, the latter only at low temperatures. As expected, with all catalysts conversion increases with increasing reaction temperature. However, different conversion trends were observed: (i) above 350 °C, the two most active catalysts are V-SBA-15 and V-MCF, with conversions at 500 °C that are approximately twice as much those of V-SBA-15-i and V-MCF-i, respectively (Table 1). Furthermore, samples obtained by direct synthesis showed higher activity than impregnated ones; (ii) above 400 °C, the non-porous V-SiO_2 sample (with V species highly dispersed and incorporated into the silica framework [8]) exhibited higher conversions than samples obtained by impregnation; (iii) below 350 °C, both V-SBA-15-i and V-MCF-i provided slightly higher conversions. Such different catalytic behaviour has to be ascribed to both different vanadium dispersion, depending on the synthesis procedure, and different support features. Moreover, it is noteworthy that above 350 °C V-SBA-15 yielded higher conversions than V-MCF and, similarly, higher performances were achieved with V-SBA-15-i with respect to V-MCF-i. The latter finding is likely due to different diffusion phenomena occurring inside the different porous structure of the two materials, as discussed below.

3.2. Catalytic activity towards propane ODH

Fig. 2a reports propane conversion in the 375–500 °C temperature range: with all the tested catalysts, a temperature increase led to higher propane conversion, mainly because of the additional contribution of propane dehydrogenation. The highest propane conversions were obtained at 500 °C with V-SBA-15-i, V-MCF-i and V-SiO_2 (Table 2), in which catalytically active sites are present at external surfaces of silica particles so that mass-transfer limitations are overcome [5,12,13]. Table 2 also gathers propene selectivity in the same conditions of temperature and time on stream (after 10 min) showing that the two samples prepared by direct synthesis were more selective at high temperature. As a whole, above 450 °C, both samples obtained by direct synthesis exhibited better selectivity to propene as compared to impregnated ones and an increase of temperature led to an increase of propene production (up to 62.0% and 67.7% at 500 °C for V-SBA-15 and V-MCF, respectively).

Fig. 2b reports propene selectivity values at about 4% conversion as obtained above 475 °C on the samples studied: V-MCF, V-SBA-15 and V-SiO_2 catalysts are more selective than impregnated ones, as consequence of the better V dispersion achieved by either direct synthesis or flame-pyrolysis method [5,8,9,12,13]. It is accepted, indeed, that isolated V species are beneficial in terms of selectivity to propene, whereas the presence polymeric VO_x groups can favour consecutive propene combustion reactions [19]. On the other hand, at low temperatures, consecutive oxidation of propene is more favoured than direct activation of propane. Therefore, the highest selectivity to propene can be obtained for systems mainly containing isolated V species and operating at high temperatures, although radical pathways take place above 550 °C [21,22].

Moreover, higher selectivity to propene was obtained over V-MCF as compared to V-SBA-15 (a similar trend was observed with impregnated samples). The latter results are likely related to the different porous networks of the two mesoporous systems. Furthermore, the non-porous sample (V-SiO_2) exhibited lower selectivity to propene, suggesting a key role of mesoporosity towards selectivity. As acknowledged by literature, in this kind of processes catalytic activity increases with V-content, but at higher V-loadings V_2O_5 segregation occurs, forming inaccessible V active centres [19]. Higher catalytic activity is ascribed to the presence of vanadate species, either isolated or polymerized up to the formation of a VO_x monolayer, whereas lower activity is usually due to the presence of bulk V_2O_5 [8]. Furthermore, simulation studies revealed that propane ODH reaction involve one-electron reduction of two V^{5+} centres to V^{4+} using one electron from each of two lattice oxygen atoms, because this mechanism requires lower activation energy than two-electron reduction (e.g. V^{5+} to V^{3+}) [20].

As far as catalysts deactivation is concerned, after 60 min on-stream at 500 °C, all catalysts presented a slight decrease of activity (such decline being more marked with impregnated catalysts), suggesting a limited deactivation of the studied systems (details not reported for brevity).

Table 2 shows that propene and CO_x were the main reaction products formed. As expected, the increase of selectivity to propene corresponds to a decrease of CO_x formation. In addition, traces of CH_4 and C_2H_4 were also observed at high temperatures (with minor differences among the studied samples), whereas oxygenated compounds such as acetone, propanal or acrolein were not detected in the 400–500 °C temperature range. Table 2 also reports propene yields at 500 °C, which are higher for impregnated samples, due to higher conversions reached when low-polymeric VO_x species are present [8,9]. Finally, in order to take into account small differences of both vanadium content and amount of sample used for the catalytic test, the production rate of propene normalized per mol of vanadium was calculated and reported in the last column of Table 2: such values are larger for impregnated samples than for

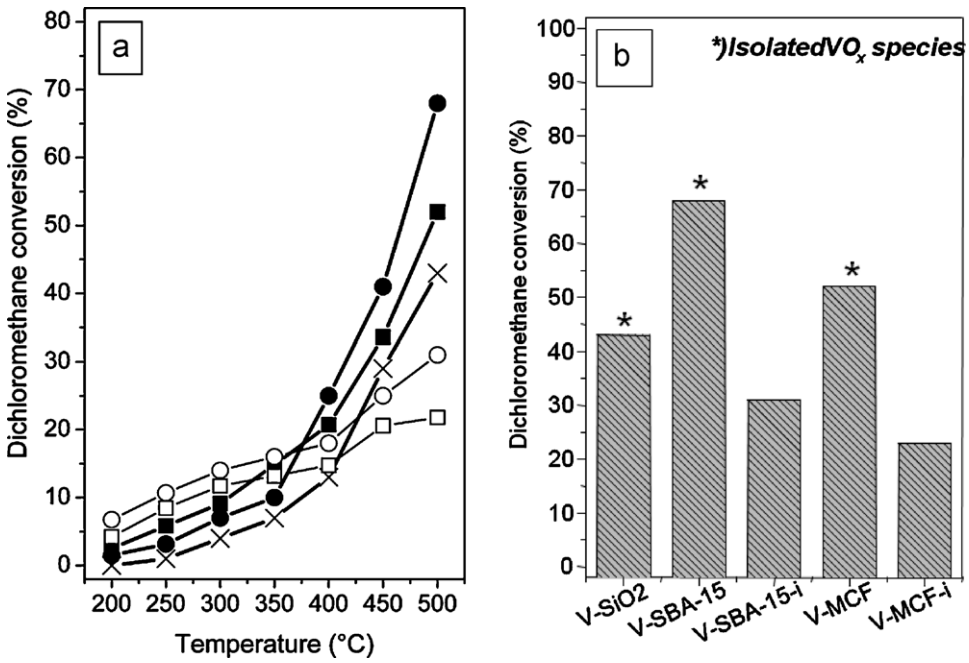

Fig. 1. Catalytic results of dichloromethane decomposition. Effect of reaction temperature on: (i) dichloromethane conversion (section a) and (ii) conversion values measured at 500 °C (section b) with V-SBA-15 (●), V-SBA-15-i (○), V-MCF (■), V-MCF-i (□) and V-SiO_2 (×) catalysts.
Adapted from Ref. [13].

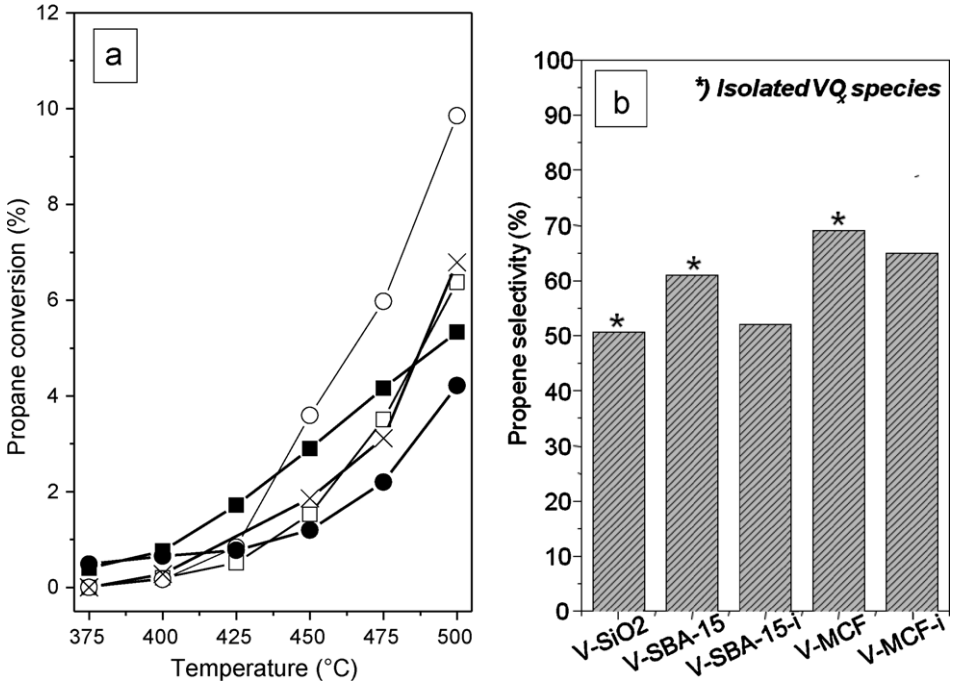

Fig. 2. Catalytic results of propane ODH. Conversions values as a function of the reaction temperature on V-SBA-15 (●), V-SBA-15-i (○), V-MCF (■), V-MCF-i (□) and V-SiO_2 (×) catalysts. Selectivity to propene (section b) at iso-conversion values (*ca.* 4% propane conv.) as measured at 500 °C.

Table 2
Catalytic data of propane ODH, as obtained at 500 °C after a time on stream of 10 min.

Sample	C_3H_8 conversion (%)	C_3H_6 selectivity (%)	ΣCH_4, C_2H_4, C_3H_4O selectivity (%)	CO_x selectivity (%)	C_3H_6 yield (%)	C_3H_6 rate (mmol/min mol V)
V-SBA-15	4.2	62.0	4.0	34.0	2.6	9.5
V-SBA-15-i	9.9	53.2	6.3	40.5	5.2	18.9
V-MCF	5.3	67.7	6.3	26.0	3.6	23.6
V-MCF-i	6.4	59.5	7.3	33.2	3.8	52.1
V-SiO_2	6.7	50.7	6.2	43.12	3.3	–

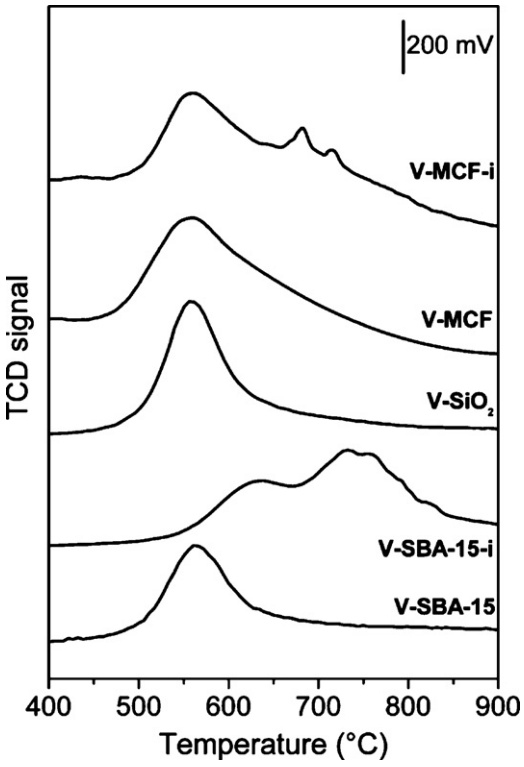

Fig. 3. H_2-TPR profiles in the 400–900 °C temperature range of the samples studied.

samples prepared by direct synthesis, since the former gave higher conversion and, furthermore, both V-MCF and V-MCF-i gave higher rates, indicating that the 3D mesoporous framework of MCF has a beneficial effect on catalytic activity in propane ODH.

3.3. *Vanadium dispersion as studied by H_2-TPR, IR and DR-UV–vis spectroscopies and TEM*

Fig. 3 reports H_2-TPR profiles in the 400–900 °C temperature range: V-SBA-15, V-MCF and V-SiO_2 samples show a main peak with a maximum at about 560 °C, readily assigned to the reduction of isolated (or at least low-polymeric) V-species. Both V-SBA-15-i and V-MCF-i profiles exhibit instead an additional reduction peak at higher temperatures (in the 600–800 °C range), due to the presence of micro-crystalline V_2O_5, typically reduced above 650 °C [5,12]. Such assignments are in agreement with micro-Raman spectroscopy analysis reported elsewhere [5,8,12,13].

Fig. 4a reports the IR spectra of powder catalysts in KBr pellets in the 1500–600 cm^{-1} range where vibrational modes of the solid absorb. The two broad bands at 1300–1100 cm^{-1} and 800 cm^{-1} are readily assigned to the asymmetric and symmetric stretch vibrations of Si–O–Si (siloxane) groups of silica, respectively [23]. It is noteworthy that with V-MCF, V-SBA-15 and V-SiO_2 samples a weak band appears at *ca.* 920 cm^{-1} (asterisk). Such band was previously observed in other V-containing silica materials (i.e. an amorphous silica and an all-silica zeolite incorporating V) [23,24] and it was assigned to the vibration of SiO_4 groups strongly polarized by the presence of framework vanadium [8]. Such band is very weak in V-MCF-i and absent in V-SBA-15-i: this confirms that a better dispersion of V species inside silica walls may be obtained if catalysts are prepared either by direct synthesis or by flame pyrolysis.

Fig. 4b reports DR UV–vis spectra of samples dehydrated at 300 °C. Spectra of V-MCF, V-SBA-15 and V-SiO_2 show a main band at *ca.* 255 nm, readily assigned to V^{5+}-O charge-transfer (CT) transitions of isolated V^{5+} species in tetrahedral coordination [5,16].

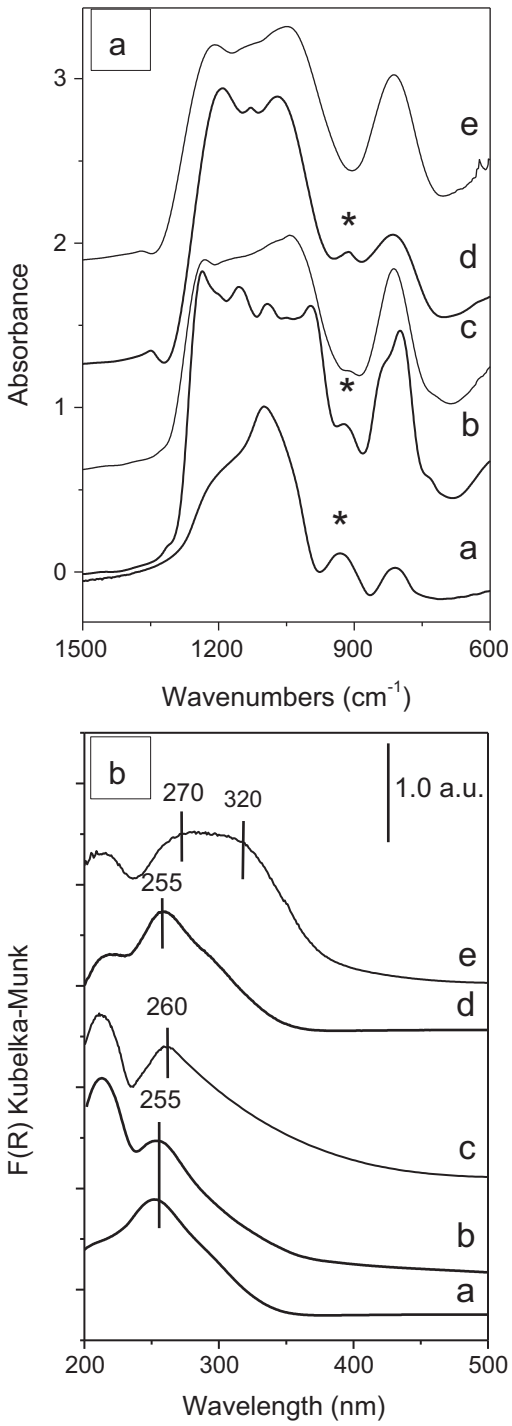

Fig. 4. Section (a): FT-IR spectra, in the 1500–600 cm^{-1} range, of samples in KBr pellets at room temperature in air. Section (b): DR UV–vis spectra of same samples outgassed for 1 h at 300 °C. In both sections: V-SiO_2 (curve a), V-MCF (curve b), V-MCF-i (curve c), V-SBA-15 (curve d) and V-SBA-15-i (curve e).

With both impregnated samples, the band of isolated V^{5+} species suffers a slight shift to *ca.* 260–270 nm, probably due to small differences in V environments [5,12] and an additional shoulder is seen at higher wavelengths (*ca.* 300–350 nm), especially with V-SBA-15-i, due to the contemporary presence of micro-crystalline vanadia. These results are in agreement with previous micro-Raman studies [5,8,12,13] and with H_2-TPR profiles discussed above.

A careful TEM analysis of SBA-15 and MCF samples was carried out and selected micrographs are reported in Fig. 5a–d. The typi-

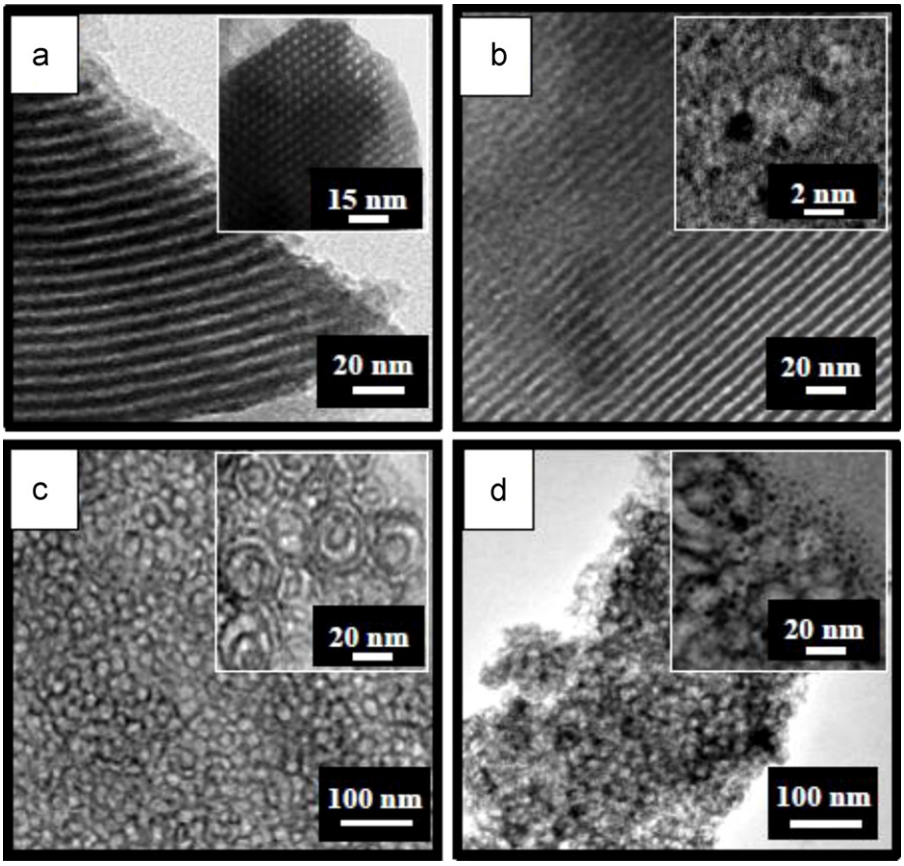

Fig. 5. TEM micrographs of V-SBA-15 (section a), V-SBA-15-i (section b), V-MCF (section c) and V-MCF-i (section d) samples.

cal morphologies of the two mesoporous systems were observed: V-SBA-15 and V-SBA-15-i showed well-ordered hexagonal arrays of mesoporous channels, whereas V-MCF and V-MCF-i showed MCF characteristic disordered array of three-dimensional mesoporous spherical cells. TEM images of the two samples prepared by impregnation (Insets to Figs. 5b and 5d) showed the occurrence of VO_x clusters at the external surface of silica particles. As a whole, TEM investigation of both V-SBA-15 and V-MCF (Fig. 5a and c, respectively) confirmed that a better dispersion and incorporation of vanadium into the silica framework was achieved by direct synthesis.

In summary, V-SBA-15, V-MCF and V-SiO_2 samples mainly show isolated V species well incorporated into silica walls, whereas with both V-SBA-15-i and V-MCF-i polymeric VO_x groups and micro-crystalline V_2O_5 [12] appear at the external surface of silica particles. These findings confirm the beneficial effect of highly dispersed (isolated) V species in both oxidation reactions. Such isolated V sites are particularly active towards oxidative decomposition of dichloromethane to CO_2, especially at high temperatures, although at low temperatures the stronger acidic properties of micro-crystalline V_2O_5 may have an effect on the catalytic activity, as discussed elsewhere [5,12,13]. On the other hand, micro-crystalline V_2O_5 may interact with dichloromethane molecules, even at low temperatures, since mass-transfer limitations are avoided at the external surfaces of particles. Similarly, the best performances in propane ODH, in terms of selectivity to propene, were obtained with catalysts prepared either by direct synthesis or by flame-pyrolysis, containing mainly isolated V active sites. Although higher activity was achieved with impregnated samples, as consequence of extra-framework micro-crystalline V_2O_5 on silica walls, these catalysts led to a smaller amount of propene in the products as measured at 4% propane iso-conversion. For both oxidation reactions, the catalytic performances of the V-SiO_2 sample were worse than those of V-MCF and V-SBA-15, although V-SiO_2 shows V species highly dispersed into the silica framework. This effect is probably related to the lower surface area of V-SiO_2 (40 $m^2\ g^{-1}$) as compared to the other mesoporous samples.

3.4. Effect of the support properties on the catalytic activity and on vanadium dispersion

Fig. 6a and b reports N_2 isotherms measured at −196 °C on mesoporous catalysts obtained by direct synthesis and impregnation, respectively. V-MCF shows type IV isotherms with H2 hysteresis loops closing at about 0.45 P/P^0, due to the empting of either "ink-bottle" mesopores or "closed cell" foams interconnected by windows and suggesting the co-presence of both MCF and MLV phases [12]. Similarly, V-SBA-15 exhibits type IV isotherms with H1 hysteresis loops, typical of SBA-15 systems and a sharp increase in the 0.4–0.5 P/P^0 range corresponding to capillary condensation within mesopores. It is noteworthy that samples prepared by direct synthesis exhibited significantly larger BET specific surface areas as compared to impregnated ones (Table 3) in which extra-framework VO_x species occur, partially occluding the overall accessible porosity. Zukal et al. [25] clearly demonstrated that the grafting of alumina on SBA-15 brings about a gradual filling of the corona surrounding the mesopores, with a consequent smoothing of mesopores surface, and a decrease of both, mesopores and external surface areas. Although in the present paper we did not carry out such a detailed porosity characterization as in Ref. [25], where

Table 3
Textural properties of the prepared samples as derived from both EDS analysis and N_2 isotherms at −196 °C.

Sample	V-content[a] (wt.%)	Synthesis method	S_{BET} ($m^2\ g^{-1}$)	D (nm)	V-density ($VO_x\ nm^{-2}$)
V-SBA-15	2.4	Direct synthesis	820	3.5[b]	0.35[e]
V-SBA-15-i	2.8	Impregnation	530	3.5[b]	0.63[e]
V-MCF	2.6	Direct synthesis	925	16[c]; 6[d]	0.33[e]
V-MCF-i	2.5	Impregnation	645	23[c]; 12[d]	0.46[e]
V-SiO_2	3.0	Flame pyrolysis	40	–	(8.89)[e]; 0.44[f]

[a] As measured by EDS analysis.
[b] Mesopores diameter as calculated according to the BJH method from isotherms desorption branch.
[c] Cells diameter as determined from adsorption branches of N_2 isotherms (BdB-FHH method).
[d] Windows diameter as determined from desorption branches of N_2 isotherms (BdB-FHH method).
[e] Vanadium dispersion as calculated by considering the vanadium content measured by EDS and the S_{BET}.
[f] Vanadium dispersion at the surface of V-SiO_2 nanoparticles, as obtained by considering H_2-TPR data.

indeed several alumina loadings were studied, it can be inferred that also in the present case a similar phenomenon may occur on V-SBA-15-i.

V-MCF-i sample exhibits similar type IV isotherms, with narrower hysteresis loops shifted to a higher relative pressure (0.60–0.90 P/P^0), indicating the presence of larger pores. The different textural properties of V-MCF and V-MCF-i are probably related to their different synthesis procedures, since the introduction of vanadium into silica walls requires less acidic conditions with respect to the synthesis of MCF silica [12].

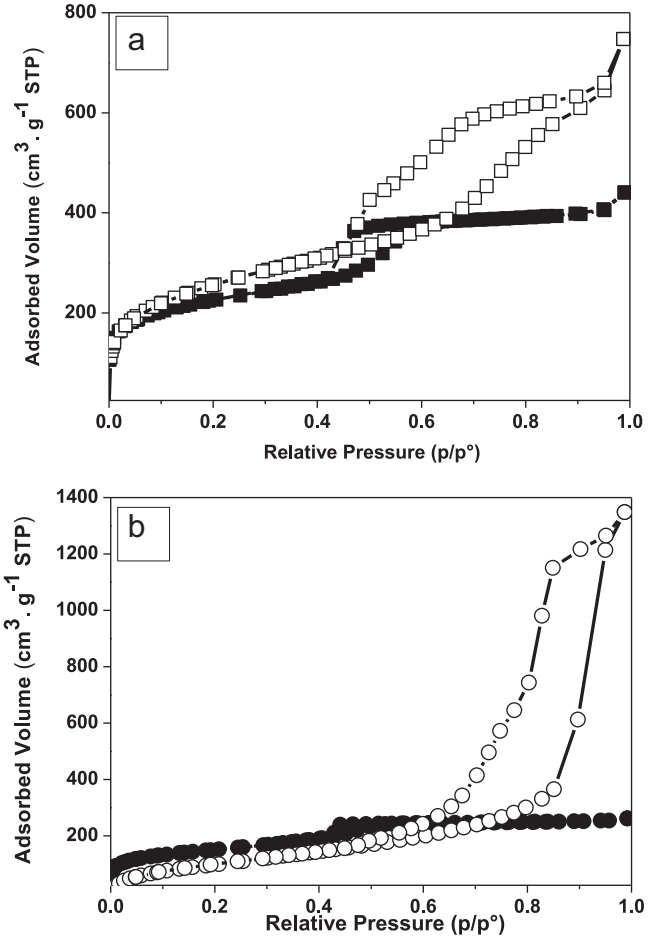

Fig. 6. N_2 adsorption/desorption isotherms measured at −196 °C on V-MCF (□) and V-SBA-15 (■) samples (section a) and V-MCF-i (○) and V-SBA-15-i (●) samples (section b).

Table 3 also reports vanadium densities (number of VO_x species per nm^2) as calculated by considering: (i) the vanadium content determined by EDS analysis and (ii) the S_{BET} on the samples studied. The obtained results clearly confirm that a better vanadium dispersion is obtained by direct synthesis, as compared to impregnation. With V-MCF-i sample, however, the vanadium density is still low, also due to the high specific surface area of this material. The result obtained in this way with V-SiO_2 sample is obviously overestimated and should not be considered, for the following reasons: (i) flame pyrolysis notoriously leads to the incorporation of vanadium inside silica nanoparticles and not only at their surface [8]; (ii) the physicochemical characterization of V-SiO_2 clearly showed that vanadium in well dispersed (see for example, DR-UV–vis spectrum). Therefore, we decided to estimate in a semi-qualitative way the amount of surface vanadium or, at least, of accessible vanadium sites on V-SiO_2 from integrated area of the only peak in its H_2-TPR profile (Fig. 3), as compared to V-SBA-15 sample. A reasonable value of 0.44 VO_x/nm^2 was obtained, confirming that flame-pyrolysis leads to very good vanadium dispersion [8] not only at the surface, but also inside silica particles.

Fig. 7 reports both TEM images of V-MCF and V-SBA-15 samples, showing their typical arrangement of mesophase: (i) V-SBA-15 exhibits a hexagonal array of mesoporous monodimensional channels that are ordered on the long range in two dimensions, as confirmed by XRD [5]; (ii) V-MCF shows a disordered array of 3D mesoporous spherical cells (*ca.* 20–25 nm) typical of MCF. Both mesoporous structures have also been schematized in the same figure, showing different diffusion of reactants and products during catalytic reactions. Specifically, the structure of mesocellular silica foams (MCF) featuring a 3-D network with large cells should favour molecules diffusion, unlike cylindrical channels (with a diameter of 3–6 nm) of SBA-15, occurring in one dimension mainly (axial diffusion). Therefore, reactants and products can be much more retained inside channels of SBA-15 as compared to ultra-large pores of 3-D MCF systems. SBA-15 structure may favour longer residence times of molecules, unlike the 3-D ultra-large pores that allow molecular diffusion along each direction inside MCF. This is in fair agreement with catalytic results obtained in both oxidation reactions at 500 °C: higher activity in dichloromethane total oxidation was obtained with V-SBA-15 as compared to V-MCF (a similar trend was observed with impregnated samples), since longer residence time of molecules favours deeper oxidation; similarly, higher selectivity to propene during ODH of propane was obtained with V-MCF and V-MCF-i, being a selective oxidation reaction. The present findings are in agreement with previous studies [26] on V-containing MCM-41 materials. The latter were demonstrated to be more active and selective in the ODH of propane with respect to VO_x catalysts supported on amorphous SiO_2, due to both higher surface area and better V-dispersion. With respect to MCM-41 materials, the larger pores of SBA-15 should favour molecular diffusion, thereby leading

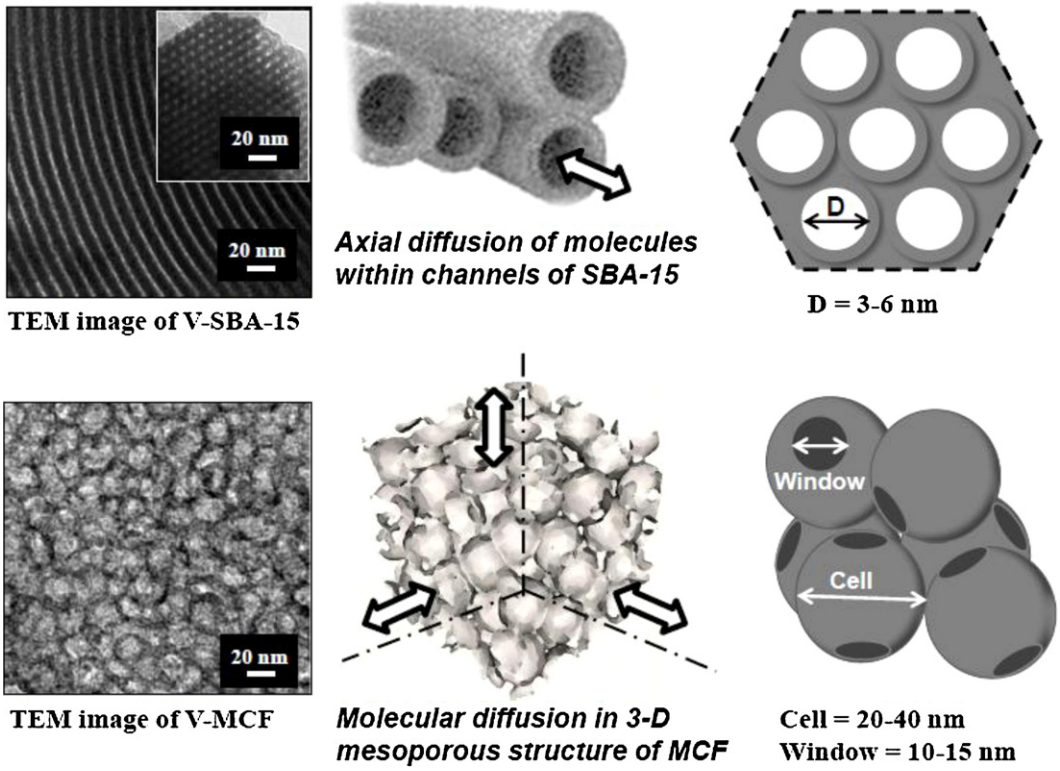

Fig. 7. TEM images and corresponding structures of V-SBA-15 sample (upper section) and V-MCF sample (lower section).

to an enhanced performance in ODH of propane. Accordingly, MCF materials with ultra-large mesopores and 3D porous structure are known to further improve molecular diffusion and to avoid deeper oxidation, as compared to both MCM-41 and SBA-15.

On the other hand, at lower reaction temperatures (e.g. below 350 °C), hydrophilic properties of catalysts play a key role in oxidation reactions. In particular, the richer hydroxyl population of materials prepared by direct synthesis and flame pyrolysis [12] may also explain their lower activity in both oxidation reactions, since water molecules produced during oxidation processes reduce the effectiveness of active centres.

4. Conclusions

The catalytic performances in both dichloromethane decomposition (a total oxidation reaction) and propane ODH (a partial oxidation reaction) were studied for vanadium–silica materials with about *ca.* 2.5 wt.% vanadium prepared by different ways and with different structures.

Concerning SBA-15 and MCF mesoporous samples, it was found that a better vanadium dispersion may be obtained by direct synthesis, rather than by impregnation, and that such a feature positively affects the catalytic activity in both kinds of (total and partial) oxidation reactions. Concerning the ODH of propane, a higher selectivity to propene was obtained with V-MCF, as compared to V-SBA-15, whereas higher dichloromethane conversions were achieved with V-SBA-15 (impregnated samples gave a similar trend). Such a different catalytic behaviour is assigned to the different porous network of the two investigated mesoporous materials: SBA-15 has monodimensional mesoporous channels that may favour longer residence times of molecules, finally promoting their total oxidation, and so V-containing SBA-15 samples were found to be more active in dichloromethane conversion. MCF has instead 3-D ultra-large pores, a structure that does favour facile molecules diffusion, this factor probably being responsible for the higher selectivity to propene achieved with both V-containing MCF catalysts in propane ODH. The important role of the mesoporous structure of the support on the catalytic activity in oxidation reactions was confirmed by the comparison with a non-porous sample ($V\text{-}SiO_2$) that, although containing well dispersed vanadium sites incorporated into the silica framework, was less active that the examined mesoporous samples.

References

[1] I.E. Wachs, Catal. Today 100 (2005) 79.
[2] P. Mars, D.W. van Krevelen, Chem. Eng. Sci. Spec. (Suppl. 3) (1954) 41.
[3] J.C. Vedrine, G. Coudurier, J.M. Millet, Catal. Today 33 (1997) 3.
[4] B.M. Weckhuysen, D.E. Keller, Catal. Today 78 (2003) 25.
[5] M. Piumetti, B. Bonelli, M. Armandi, L. Gaberova, S. Casale, P. Massiani, E. Garrone, Microporous Mesoporous Mater. 133 (2010) 36.
[6] X. Gao, I.E. Wachs, Top. Catal. 18 (2002) 243.
[7] F. Cavani, N. Ballarini, E. Cericola, Catal. Today 127 (2007) 113.
[8] I. Rossetti, L. Fabbrini, N. Ballarini, F. Cavani, A. Cericola, B. Bonelli, M. Piumetti, E. Garrone, H. Dyrbeck, E.A. Blekkan, L. Forni, J. Catal. 256 (2008) 45.
[9] I. Rossetti, L. Fabbrini, N. Ballarini, C. Oliva, F. Cavani, A. Cericola, B. Bonelli, M. Piumetti, E. Garrone, H. Dyrbeck, E.A. Blekkan, L. Forni, J. Catal. 141 (2009) 271.
[10] I. Muylaert, P. Van Der Voort, Phys. Chem. Chem. Phys. 11 (2009) 2826.
[11] A. Taguchi, F. Schüth, Microporous Mesoporous Mater. 77 (2005) 1.
[12] M. Piumetti, B. Bonelli, P. Massiani, Y. Millot, S. Dzwigaj, M. Armandi, L. Gaberova, E. Garrone, Microporous Mesoporous Mater. 142 (2011) 45.
[13] M. Piumetti, B. Bonelli, P. Massiani, S. Dzwigaj, I. Rossetti, S. Casale, L. Gaberova, M. Armandi, E. Garrone, Catal. Today doi:10.1016/j.cattod.2010.10.066.
[14] F. Ying, J. Li, C. Huang, W. Weng, H. Wan, Catal. Lett. 115 (2007) 137.
[15] Y.-M. Liu, W. -L- Feng, T.-C. Li, H.-Y. He, W.-L. Dai, W. Huang, Y. Cao, K.-N. Fan, J. Catal. 239 (2006) 125.
[16] F. Gao, Y. Zhang, H. Wan, Y. Kong, X. Wu, L. Dong, B. Li, C. Yi, Microporous Mesoporous Mater. 110 (2008) 508.
[17] G. Ertl, H. Knözinger, F. Schüth, J. Weitkamp, Handbook of Heterogeneous Catalysis , 2nd ed., Wiley, John & Sons Incorporated, 2008, p. 2397.
[18] J. Haber, T. Machej, M. Derewiński, R. Janik, J. Kryściak, H. Sadowska, J. Janas, Catal. Today 54 (1999) 47.
[19] N. Ballarini, F. Cavani, A. Cericola, Catal. Today 127 (2007) 113.

[20] F. Gilardoni, A.T. Bell, A. Chakraborty, P. Boulet, J. Phys. Chem. B 104 (2000) 12250.
[21] G. Mul, M.A. Banares, G. Garcia Cortez, B. van der Linden, S.J. Khatib, J.A. Moulijn, Phys. Chem. Chem. Phys. 5 (2003) 4378.
[22] M.D. Argyle, K. Chen, A.T. Bell, E. Iglesia, J. Catal. 208 (2002) 139.
[23] S. Dzwigaj, P. Massiani, A. Davidson, M. Che, J. Mol. Catal. A: Chem. 155 (2000) 169.
[24] D.E. Keller, T. Visser, F. Soulimani, D.C. Koninsberger, B.M. Weckhuysen, Vib. Spectrosc. 43 (2007) 140.
[25] A. Zukal, H. Siklová, J. Cejka, Langmuir 24 (2008) 9837.
[26] Y.M. Liu, W.L. Feng, T.C. Li, H.Y. He, W.L. Dai, W. Huang, Y. Cao, K.N. Fan, J. Catal. 239 (2006) 125.